



TITLE:

Some Physical Properties of BiO.-BaO-CuO Glasses (Commemoration Issue Dedicated to Professor Sumio Sakka On the Occasion of His Retirement)

AUTHOR(S):

Miyaji, Fumiaki; Fujimine, Satoshi; Yoko, Toshinobu; Sakka, Sumio

CITATION:

Miyaji, Fumiaki ...[et al]. Some Physical Properties of BiO.-BaO-CuO Glasses (Commemoration Issue Dedicated to Professor Sumio Sakka On the Occasion of His Retirement). Bulletin of the Institute for Chemical Research, Kyoto University 1994, 72 ...

ISSUE DATE:

1994-10-31

URL:

<http://hdl.handle.net/2433/77574>

RIGHT:

Some Physical Properties of $\text{BiO}_{1.5}\text{-BaO-CuO}$ Glasses

Fumiaki MIYAJI*, Satoshi FUJIMINE**,
Toshinobu YOKO*** and Sumio SAKKA***

Received May 27, 1994

The density, refractive index, glass-transition temperature and crystallization temperature were investigated for $\text{BiO}_{1.5}\text{-BaO-CuO}$ ternary glasses in relation to copper valence and glass structure. It was found that the $\text{Cu}^+ \text{-Cu}^{2+}$ equilibrium moves toward reduction side (Cu^+) with increasing melting temperature and the BaO content. Judging from the additivity of the measured properties, the glass structure hardly changes with glass composition when $\text{Cu}^+ / (\text{Cu}^+ + \text{Cu}^{2+})$ ratio is constant. On the other hand, the glass structure might be more open structure at the $\text{Cu}^+ / (\text{Cu}^+ + \text{Cu}^{2+})$ ratio higher than 60%. The molar volume and refractive index of fictive Bi_2O_3 glass estimated by extrapolation are almost the same as those of $\alpha\text{-Bi}_2\text{O}_3$ crystal. The local structure around Bi^{3+} ions were therefore assumed to resemble that in $\alpha\text{-Bi}_2\text{O}_3$ crystal. The Cu_4O_3 crystal-like structural units might also be present in the Bi-Ba-Cu-O glasses, contributing to wide glass-forming region in the present system.

KEY WORDS : $\text{BiO}_{1.5}\text{-BaO-CuO}$ glasses/ Density/ Molar volume/ Refractive index/ $\text{Cu}^+ \text{-Cu}^{2+}$ equilibrium/ Glass structure

1. INTRODUCTION

Since Komatsu *et al.* found that Bi-Sr-Ca-Cu-O composition corresponding to high T_c superconductor form a glass by ordinary melt quenching technique,¹⁾ those and related glasses containing Bi_2O_3 , CuO and alkaline earth oxides (CaO, SrO and/or BaO) have attracted an attention not only as a precursor of superconductors but also as a new family of so-called "non-conventional" oxide glasses.

There have been many studies on preparation of Bi-Sr-Ca-Cu-O superconductor ceramics by crystallizing the melt-quenched glasses.¹⁻⁵⁾ On the other hand, several researchers investigated the structure and properties of the glasses. Zheng *et al.* measured the density, glass-transition temperature and crystallization onset temperature of Bi-Sr-Ca-Cu-O glasses and presumed their structure by infrared spectroscopy.⁶⁾ Moreover, specific heat,⁷⁾ viscosity,⁸⁾ and electrical conduction⁹⁾ have been investigated for the glasses so far.

It is, however, difficult to clarify the compositional dependence of structure and properties of Bi-Sr-Ca-Cu-O glasses, since they consists of four kinds of oxides. For simplified analysis, the present authors determined the glass-forming regions in the $\text{BiO}_{1.5}\text{-CaO-CuO}$,¹⁰⁾ $\text{BiO}_{1.5}\text{-SrO-CuO}$ ¹⁰⁾ and $\text{BiO}_{1.5}\text{-BaO-CuO}$ ¹¹⁾ ternary systems and investigated the structure and properties of these glasses. It was suggested that glass structure of these three systems may be considerably

* 宮路史明 : Division of Material Chemistry, Faculty of Engineering, Kyoto University, Kyoto 606-01, Japan.

** 藤峰 哲 : Asahi Glass Company, Kanagawa-ku, Yokohama 221, Japan.

*** 横尾俊信, 作花濟夫 : Institute for Chemical Research, Kyoto University, Uji, Kyoto-fu 611, Japan.

different one another.^{10,11)} On the other hand, Sato *et al.* examined the crystallization behavior of Bi₂Sr₂CuO_x glasses.¹²⁾

Taking into consideration that the glass-forming region in the Bi-Ba-Cu-O system is widest among all the Bi-R-Cu-O ternary systems, the Bi-Ba-Cu-O system will be most appropriate in order to clarify the compositional dependence of properties of the BiO_{1.5}- and CuO-based glass systems. The authors have already studied the crystallization behavior^{11,13,14)} and electrical conduction¹⁵⁾ of Bi-Ba-Cu-O glasses. In the present work, some physical properties viz. the density, refractive index, glass-transition and crystallization temperatures were studied in relation to the valence state of copper ions and the glass structure.

2. EXPERIMENTAL

2.1 Sample preparation

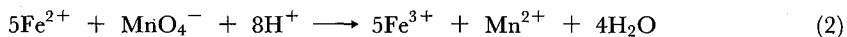
Bi-Ba-Cu-O glasses with various compositions and Bi₂Sr₂CaCu₂O_x glass were prepared. 10 g well-mixed glass batches containing of reagent-grade Bi₂O₃, RCO₃ (R=Ca, Sr, Ba) and CuO were melted in a high-grade alumina crucible with a lid in an electric furnace at 1,250°C for the Bi₂Sr₂CaCu₂O_x composition and at 1,350°C for the Bi-Ba-Cu-O systems for 10 min. The melt was poured onto a brass plate and quickly pressed by another plate. Black-colored glasses were obtained. Glasses of some compositions were also prepared in a similar manner but at various melting temperatures (950–1,350°C), in order to realize wide variations of Cu⁺/(Cu⁺+Cu²⁺) ratio in the glasses.

2.2 Determination of copper valence

The valence state of copper ions in the glasses was determined by the following technique. First, Cu⁺ was determined by potential-difference titration. About 0.1 g glass sample was dissolved in an aqueous solution containing Fe₂(SO₄)₃·H₂O and HCl. In this process, Cu⁺ is oxidized to Cu²⁺.



Another aqueous solution containing MnSO₄·4H₂O, H₂SO₄ and H₃PO₄ was added to the solution to avoid yellow-coloration of Fe³⁺ and the interference of titration by the presence of Cl[−]. Fe²⁺ produced by eq. (1) were determined by back-titration using 0.01 M KMnO₄ solution.



The end point was determined as the inflection point of potential curve.

Next Cu²⁺ was determined by iodometric titration. Excess KI was added to 1 M HCl solution and about 0.1 g glass sample was dissolved in this solution.



I₂ produced by eq. (3) was determined by back titration using 0.01 M Na₂S₂O₃ solution.



Just before the end point, the starch solution as indicator was added to the solution. The end point was determined as the point that the color of the solution was changed from purple to

colorless. N_2 gas was bubbled in the solution during the above operation to avoid the air-oxidation of Cu^+ and I^- .

2.3 Density and refractive index

The densities of the glasses were measured by Archimedeian method using kerosene as an immersion liquid. The refractive indices were measured on the series of $(100-3x)BiO_{1.5} \cdot BaO \cdot 2xCuO$ ($x=5, 10, 20$) glasses. The glass sample was polished to 0.1–0.2 mm thick. A Mizojiri-Kogaku model DVA-36VW ellipsometer was employed in order to measure the refractive index in the range 500–1,050 nm.

2.4 Thermal analyses

The glass transition temperature, T_g , and the crystallization onset temperature, T_x , of the glasses with various $Cu^+/(Cu^+ + Cu^{2+})$ ratio were measured by a Rigaku-Denki model Thermoflex TG 8110 DSC/DTA apparatus. The measurements were performed on bulk samples of about 40 mg under an air atmosphere.

3. RESULTS

3.1 Copper valence

Figure 1 shows the results of valence determination of copper ions in the $(100-2x)BiO_{1.5} \cdot BaO \cdot CuO$ glasses melted at $1,350^\circ C$. It is found that $Cu^+/(Cu^+ + Cu^{2+})$ ratio (a) is almost constant around 75%. Figure 2 shows the variation of the $Cu^+/(Cu^+ + Cu^{2+})$ ratio in $50BiO_{1.5} \cdot 25BaO \cdot 25CuO$, $60BiO_{1.5} \cdot 10BaO \cdot 30CuO$ and $80BiO_{1.5} \cdot 5BaO \cdot 15CuO$ glasses as a function of melting temperature. As to all the compositions, the $Cu^+/(Cu^+ + Cu^{2+})$ ratio increases with increasing melting temperature and most of copper ions are present as Cu^+ for the

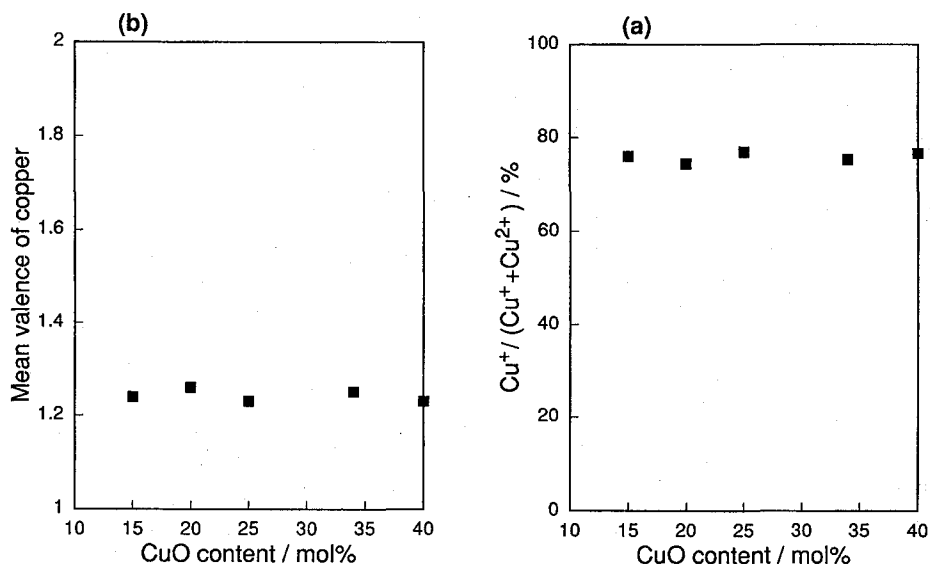


Fig. 1. (a) $Cu^+/(Cu^+ + Cu^{2+})$ ratio and (b) mean valence of copper as a function of CuO content for $(100-2x)BiO_{1.5} \cdot xBaO \cdot xCuO$ glasses. The melting temperature was fixed at $1,350^\circ C$ for all the glasses.

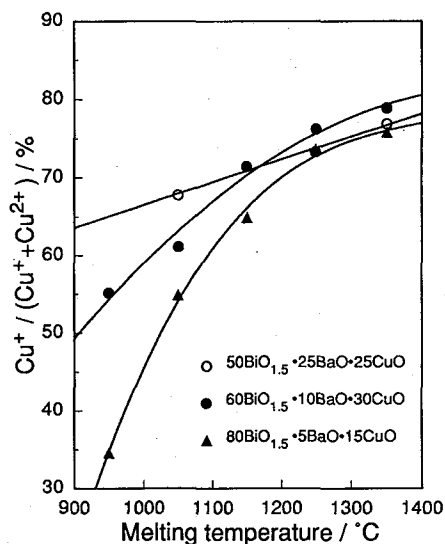


Fig. 2. Variation of $\text{Cu}^+ / (\text{Cu}^+ + \text{Cu}^{2+})$ ratio in $50\text{BiO}_{1.5}\cdot 25\text{BaO}\cdot 25\text{CuO}$, $60\text{BiO}_{1.5}\cdot 10\text{BaO}\cdot 30\text{CuO}$ and $80\text{BiO}_{1.5}\cdot 5\text{BaO}\cdot 15\text{CuO}$ glasses as a function of melting temperature.

melting temperatures higher than $1,250^\circ\text{C}$. It is also found that the higher the BaO content, the higher the $\text{Cu}^+ / (\text{Cu}^+ + \text{Cu}^{2+})$ ratio at lower temperatures than $1,100^\circ\text{C}$.

3.2 Density and refractive index

The density and molar volume of $\text{BiO}_{1.5}\text{-BaO-CuO}$ glasses are listed in Table 1, in which V_m and V_o denote the molar volume per one total-cation mol and per one oxygen mol, respectively.

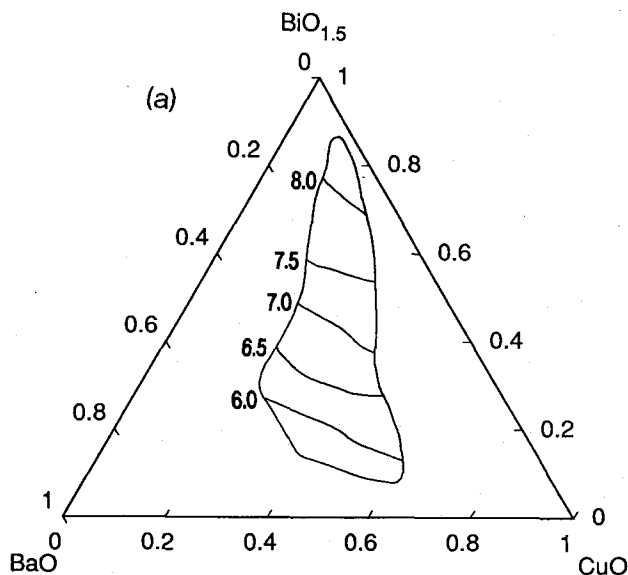


Fig. 3

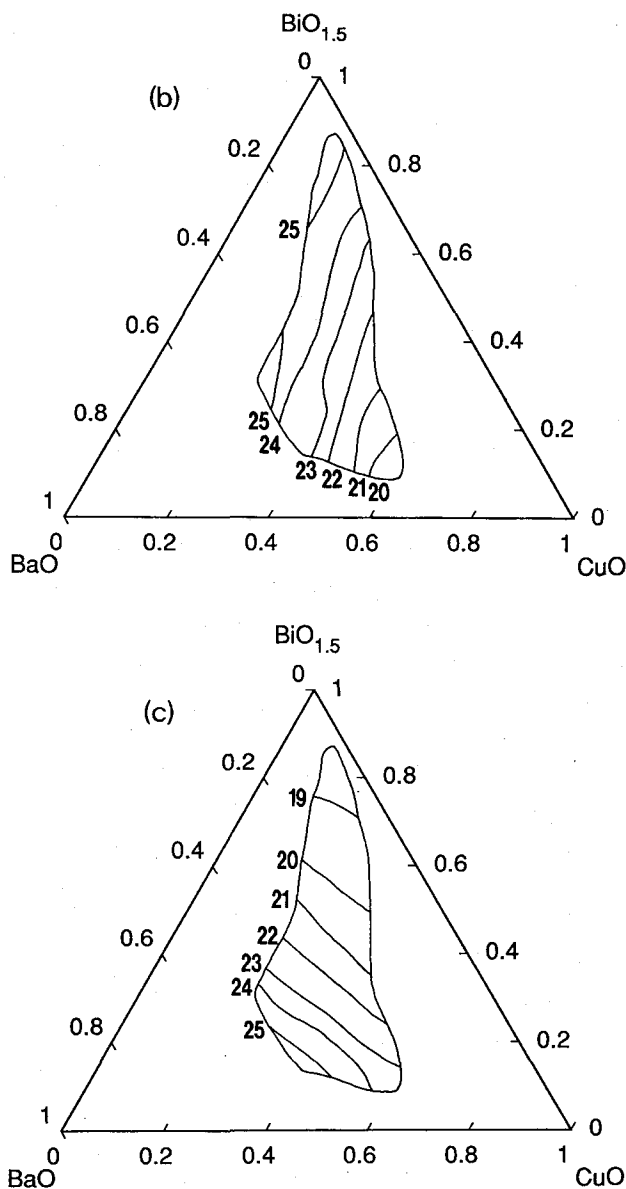


Fig. 3. Contours of (a) density, (b) V_m and (c) V_o in $\text{BiO}_{1.5}$ - BaO - CuO glasses.

In calculation, the $\text{Cu}^+ / (\text{Cu}^+ + \text{Cu}^{2+})$ ratio is fixed at 0.75 based on the results in figure 1(a). Figure 3 shows the contours of (a) density, (b) V_m and (c) V_o in $\text{BiO}_{1.5}$ - BaO - CuO glasses. It is found that the density increases and decreases with increasing $\text{BiO}_{1.5}$ and BaO contents, respectively and that V_m decreases with increasing CuO content and V_o decreases with increasing $\text{BiO}_{1.5}$ content.

Figure 4 shows the (a) density, (b) V_m and (c) V_o in $\text{Bi}_2\text{Sr}_2\text{CaCu}_2\text{O}_x$, $60\text{BiO}_{1.5}\cdot 10\text{BaO}\cdot 30\text{CuO}$ and $80\text{BiO}_{1.5}\cdot 5\text{BaO}\cdot 15\text{CuO}$ glasses as a function of $\text{Cu}^+ / (\text{Cu}^+ + \text{Cu}^{2+})$ ratio. The density and

Some Physical Properties of BiO_{1.5}-BaO-CuO Glasses

Table 1. Density and molar volume of BiO_{1.5}-BaO-CuO glasses.

Composition			d/gcm^{-3}	$V_m/\text{cm}^3\text{mol}^{-1}$	$V_o/\text{cm}^3\text{mol}^{-1}$
Bi	Ba	Cu			
10	30	60	5.848	19.37	23.48
15	45	40	5.652	23.60	25.51
17	33	50	6.042	21.02	23.42
20	30	50	6.217	20.81	22.81
20	40	40	5.886	23.34	24.57
25	45	30	5.968	25.02	24.71
30	25	45	6.613	21.37	21.78
30	30	40	6.568	22.12	22.12
30	40	30	6.398	23.96	23.09
30	45	25	6.148	25.58	24.22
33.3	33.3	33.4	6.594	23.13	22.29
35	25	40	6.761	22.08	21.54
40	20	40	7.048	21.75	20.71
40	30	30	6.755	23.87	21.94
40	35	25	6.733	24.54	22.18
50	15	35	7.394	22.35	19.98
50	20	30	7.296	23.19	20.39
50	25	25	7.172	24.15	20.89
55	15	30	7.544	22.96	19.75
60	10	30	7.737	22.90	19.28
60	15	25	7.623	23.77	19.71
60	20	20	7.561	24.49	19.99
70	10	20	7.910	24.41	19.15
70	15	15	7.878	25.02	19.34
75	10	15	7.993	25.16	19.08
80	5	15	8.259	24.83	18.48
85	5	10	8.437	25.25	18.25

¹⁾ V_m ; molar volume per one total-cation mol, ²⁾ V_o ; molar volume per one oxygen mol, ³⁾ Melting temperature was fixed at 1,350°C for all the compositions, ⁴⁾ $\text{Cu}^+ / (\text{Cu}^+ + \text{Cu}^{2+})$ ratio is fixed at 0.75 in calculation.

the molar volume decreases and increases with increasing the $\text{Cu}^+ / (\text{Cu}^+ + \text{Cu}^{2+})$ ratio, respectively.

Figure 5 shows the wavelength dependence of refractive index in $(100-3x)\text{BiO}_{1.5} \cdot \text{BaO} \cdot 2x\text{CuO}$ ($x=5, 10, 20$) glasses. It is found that the refractive index becomes higher as the $\text{BiO}_{1.5}$ content increases.

3.3 Thermal analysis

Figure 6 shows the DSC curves of $80\text{BiO}_{1.5} \cdot 5\text{BaO} \cdot 15\text{CuO}$ glass prepared at various melting temperatures. It is found that T_g , T_x and T_p decreases with increasing melting temperature. Figure 7 shows the (a) T_g and (b) $(T_x - T_g)$ in $\text{Bi}_2\text{Sr}_2\text{CaCu}_2\text{O}_x$, $50\text{BiO}_{1.5} \cdot 25\text{BaO} \cdot 25\text{CuO}$, $60\text{BiO}_{1.5} \cdot 10\text{BaO} \cdot 30\text{CuO}$ and $80\text{BiO}_{1.5} \cdot 5\text{BaO} \cdot 15\text{CuO}$ glasses as a function of $\text{Cu}^+ / (\text{Cu}^+ + \text{Cu}^{2+})$ ratio. It is found that $(T_x - T_g)$ shows the maximum at 55–65% of $\text{Cu}^+ / (\text{Cu}^+ + \text{Cu}^{2+})$ ratio.

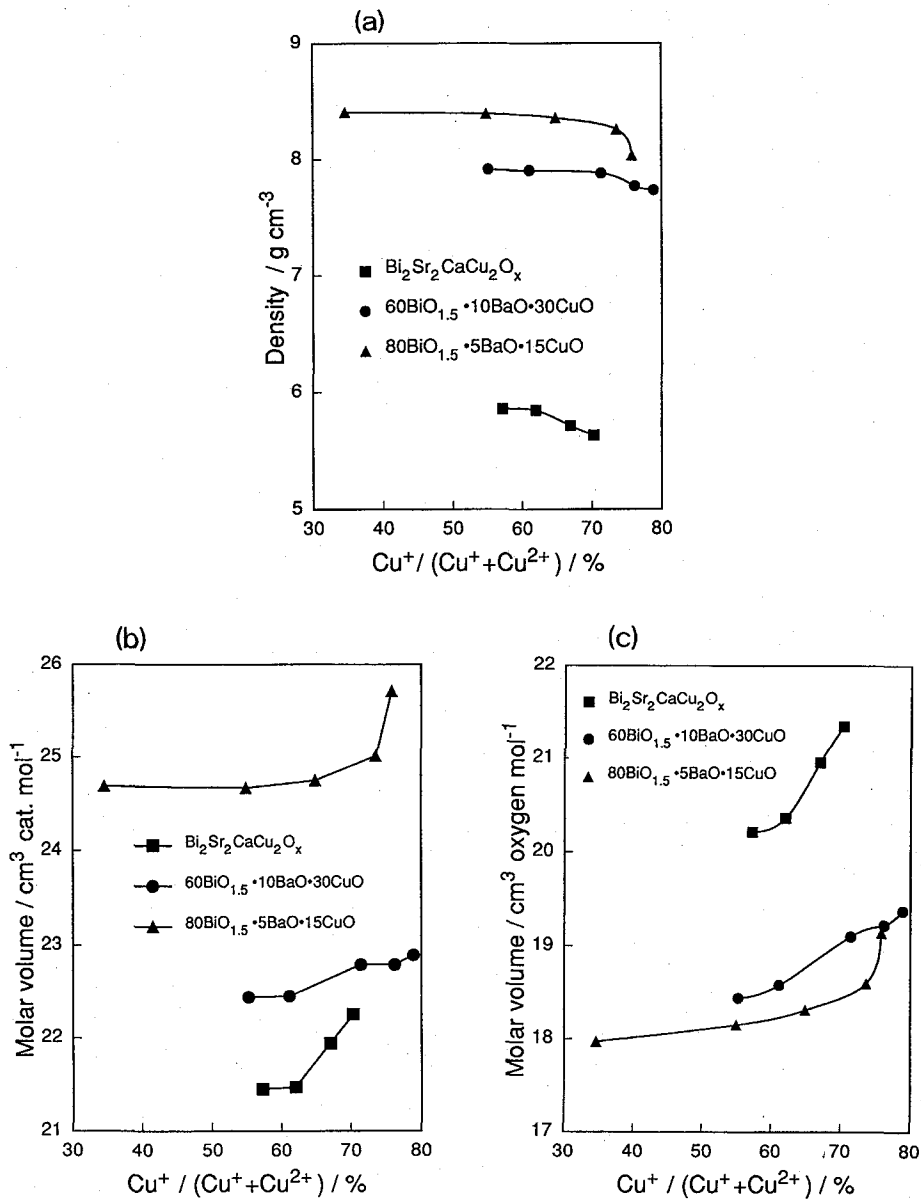


Fig. 4. (a) density, (b) V_m and (c) V_o in $\text{Bi}_2\text{Sr}_2\text{CaCu}_2\text{O}_x$, $60\text{BiO}_{1.5} \cdot 10\text{BaO} \cdot 30\text{CuO}$ and $80\text{BiO}_{1.5} \cdot 5\text{BaO} \cdot 15\text{CuO}$ glasses as a function of $\text{Cu}^+ / (\text{Cu}^+ + \text{Cu}^{2+})$ ratio.

4. DISCUSSION

4.1 $\text{Cu}^+ - \text{Cu}^{2+}$ equilibrium

It is found that the $\text{Cu}^+ / (\text{Cu}^+ + \text{Cu}^{2+})$ ratio increases with increasing melting temperature, agreeing with other copper-containing oxide glasses such as $30\text{Na}_2\text{O} \cdot 70\text{B}_2\text{O}_3$,¹⁶⁾ $30\text{R}_2\text{O} \cdot 70\text{SiO}_2$ ($\text{R} = \text{alkali metal}$),¹⁷⁾ $15\text{Na}_2\text{O} \cdot 10\text{Al}_2\text{O}_3 \cdot 75\text{B}_2\text{O}_3$,¹⁸⁾ $19.2\text{Na}_2\text{O} \cdot 4\text{CaO} \cdot 76.8\text{SiO}_2$,¹⁹⁾ and $\text{Bi}_4\text{Sr}_3\text{Ca}_3\text{Cu}_4\text{O}_x$ ²⁰⁾ glasses.

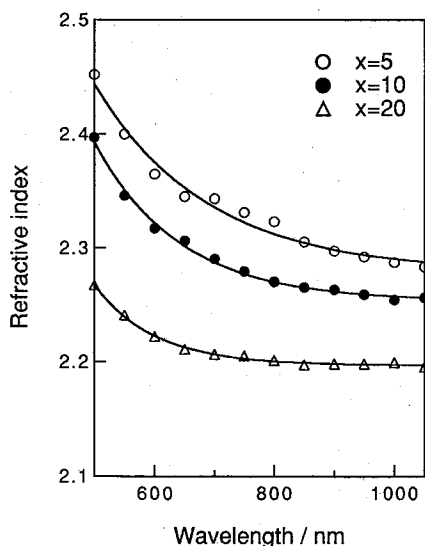


Fig. 5. Wavelength dependence of refractive index in $(100-3x)\text{BiO}_{1.5}\cdot x\text{BaO}\cdot 2x\text{CuO}$ ($x=5, 10, 20$) glasses. The melting temperature was fixed at $1,350^\circ\text{C}$ for all the glasses.

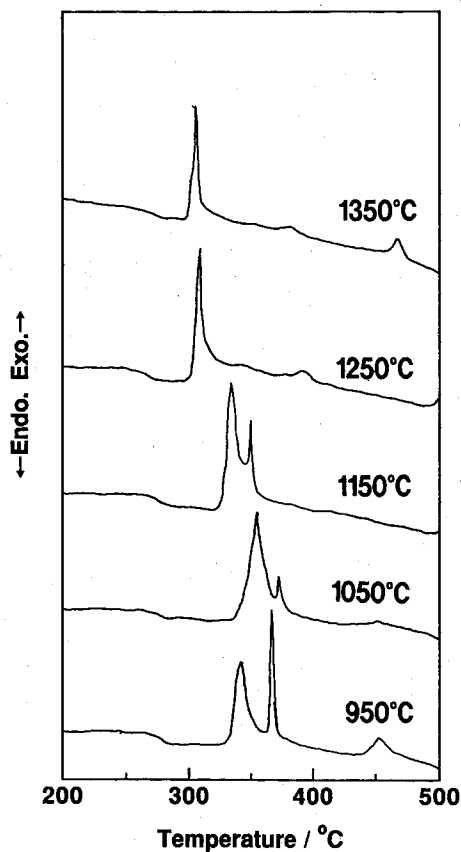


Fig. 6. DSC curves of $80\text{BiO}_{1.5}\cdot 5\text{BaO}\cdot 15\text{CuO}$ glass prepared at various melting temperatures. The heating rate is $10^\circ\text{C}/\text{min}$.

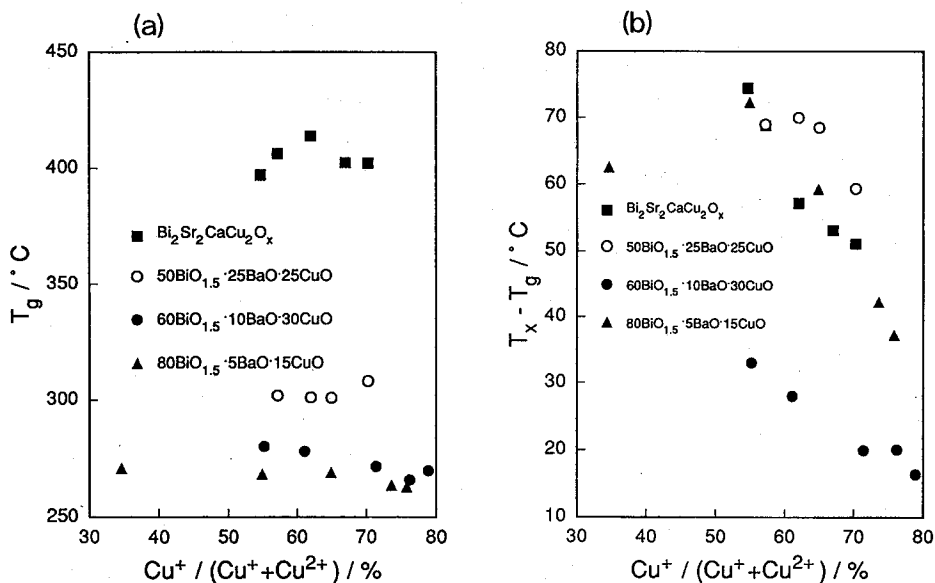


Fig. 7. (a) T_g and (b) $(T_x - T_g)$ in $\text{Bi}_2\text{Sr}_2\text{CaCu}_2\text{O}_x$, $50\text{BiO}_{1.5}\cdot 25\text{BaO}\cdot 25\text{CuO}$, $60\text{BiO}_{1.5}\cdot 10\text{BaO}\cdot 30\text{CuO}$ and $80\text{BiO}_{1.5}\cdot 5\text{BaO}\cdot 15\text{CuO}$ glasses as a function of $\text{Cu}^+ / (\text{Cu}^+ + \text{Cu}^{2+})$ ratio.

It is also seen that the $\text{Cu}^+ \text{-} \text{Cu}^{2+}$ equilibrium moves toward reduction side (Cu^+) with increasing BaO content, which is consistent with the case for copper ions in $30\text{R}_2\text{O} \cdot 70\text{SiO}_2$ glass with various R_2O content.¹⁷⁾ Singh *et al.* expressed the equilibrium of copper ions in the melt as follows.¹⁸⁾



The equilibrium constant of the above equation is therefore expressed by

$$K = \frac{[\text{Cu}^{2+}](a_{\text{O}^{2-}})^{1/2}}{[\text{Cu}^+]^{1/2}(p\text{O}_2)^{1/4}} \quad (6)$$

The activity of O^{2-} ions, $a_{\text{O}^{2-}}$, is assumed to increase with increasing BaO content, since the Ba-O bond is more ionic compared with the Bi-O and Cu-O bonds. That is, the $\text{Cu}^+ \text{-} \text{Cu}^{2+}$ equilibrium moves toward reduction side with increasing basicity²¹⁾ of glass.

4.2 Density

Figure 8 shows the relation between the V_m and $\text{BiO}_{1.5}$ content in $\text{BiO}_{1.5}\text{-BaO-CuO}$ glasses. The linear relation holds for all the Ba/Cu series, indicating the additivity of V_m in the pseudobinary $\text{BiO}_{1.5}\text{-(Ba,Cu)}_2\text{O}_2$ system. This also suggests that the local structure around Bi^{3+} ions does not significantly change with glass composition. The average V_m of single $\text{BiO}_{1.5}$ glass estimated by extrapolation for each line is $26.7 \text{ cm}^3 \text{ mol}^{-1}$, which is slightly larger than V_m of $\alpha\text{-Bi}_2\text{O}_3$ crystal, viz. $25.32 \text{ cm}^3 \text{ mol}^{-1}$.²²⁾ This indicates that the packing around Bi^{3+} ions is not denser in the present glasses than in $\alpha\text{-Bi}_2\text{O}_3$ crystal. However, the small difference in the V_m values between them may indicate that Bi^{3+} ions are present as BiO_5 or BiO_6 form as in $\alpha\text{-Bi}_2\text{O}_3$ crystal, similarly to $\text{BiO}_{1.5}\text{-GaO}_{1.5}$ glass.²³⁾

Figure 9 shows the calculated V_m for fictive BaO-CuO binary glasses as a function of

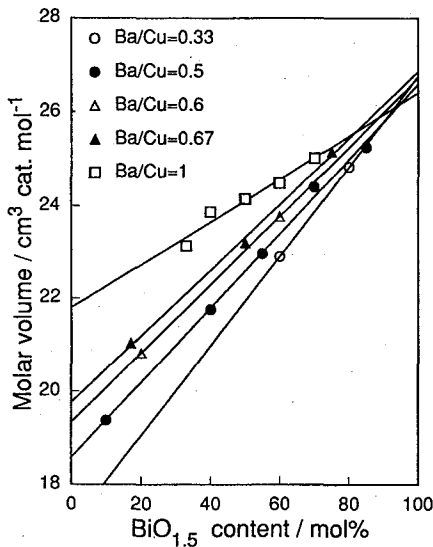


Fig. 8. Relation between the V_m and $\text{BiO}_{1.5}$ content in $\text{BiO}_{1.5}\text{-BaO-CuO}$ glasses for various Ba/Cu ratio. These data correspond to ones in Table 1.

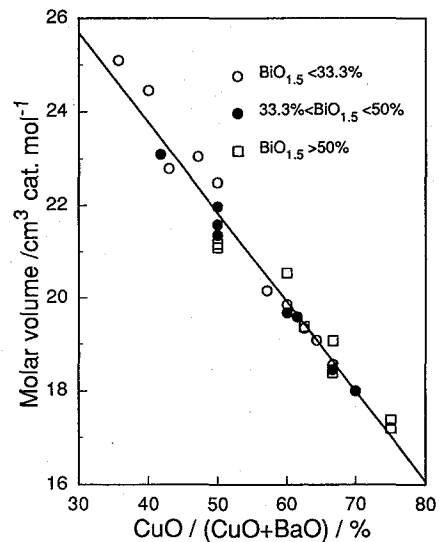


Fig. 9. V_m of fictive BaO-CuO binary glasses as a function of $\text{CuO}/(\text{CuO}+\text{BaO})$ ratio. The V_m of single $\text{BiO}_{1.5}$ is fixed at $26.7 \text{ cm}^3 \text{ mol}^{-1}$ in calculation.

CuO/(CuO+BaO) ratio. It is found that V_m does not depend on BiO_{1.5} content and the V_m linearly decreases with increasing CuO/(CuO+BaO) ratio, where the V_m of BiO_{1.5} is fixed at 26.7 cm³mol⁻¹. This suggests that the coordination environments around Cu²⁺ and Ba²⁺ ions are hardly affected by glass composition.

As shown in figure 4(b), V_m is nearly constant up to 60% of Cu⁺/(Cu⁺+Cu²⁺) ratio and starts to increase from this point. It may be explained by assuming that oxygen atoms are eliminated without the change in configuration of cations up to 60% of Cu⁺/(Cu⁺+Cu²⁺) ratio, whereas at Cu⁺/(Cu⁺+Cu²⁺) ratio higher than 60% of copper ions rearrange resulting in the increase in V_m . As a result, more open glass structure may be realized in high Cu⁺/(Cu⁺+Cu²⁺) region. The coordination of copper ions will be discussed later.

4.3 Refractive index

The high refractive index (>2.2) of the present glasses is ascribed to high concentration of Bi³⁺ ions with high polarizability. According to Wemple,²⁴⁾ the following equation holds at high photon energies,

$$\frac{1}{n^2-1} = \frac{E_0}{E_d} - \frac{E^2}{E_0 E_d} \quad (7)$$

where E , E_0 and E_d represent the photon energy, the average excitation energy and the electronic oscillation strength, respectively. Figure 10 shows the relation between $1/(n^2-1)$ and E^2 . As expected from eq. (7), the linear relationship between $1/(n^2-1)$ and E^2 is seen for all the compositions. The refractive index at any wavelength can be therefore estimated from interpolation or extrapolation of these straight lines. Table 2 lists the refractive index at various wavelengths, Abbe number, ν_d , and molar refraction, R_m . The n_d , n_F , n_C and n_∞ represent refractive indices at the wavelengths of 587.6, 486.1, 656.3 nm and infinity, respectively. The R_m is calculated by

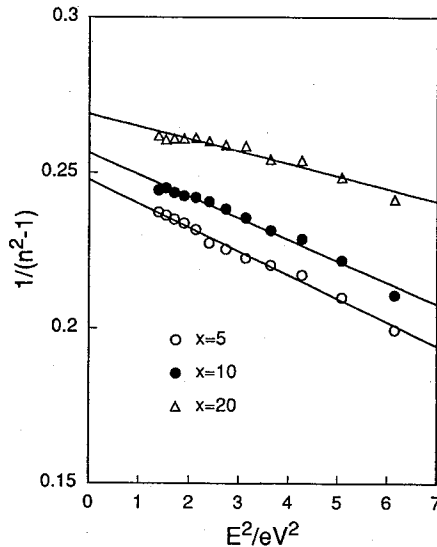
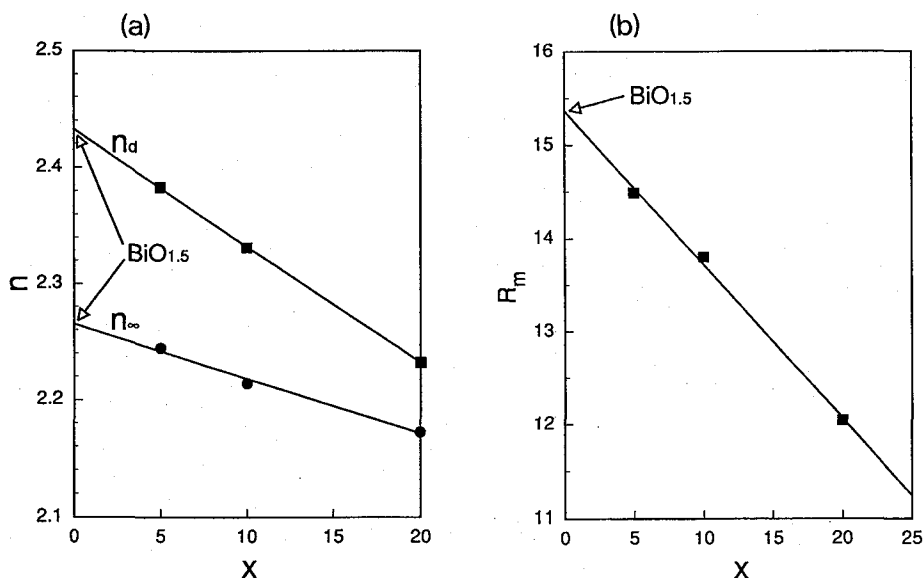


Fig. 10. Plot of $1/(n^2-1)$ vs. E^2 for $(100-3x)\text{BiO}_{1.5} \cdot x\text{BaO} \cdot 2x\text{CuO}$ glasses. The melting temperature was fixed at 1,350°C for all the glasses.

Table 2. Refractive index (n), Abbe number (ν) and molar refraction (R_m) of $(100-3x)\text{BiO}_{1.5}\cdot x\text{BaO}\cdot 2x\text{CuO}$ glasses.

x	n_d	n_F^*	n_C	ν_d	n_{∞}^*	$R_m/\text{cm}^3\text{mol}^{-1}$
0*	2.43				2.27	15.4
5	2.38	2.46	2.35	13.0	2.24	14.5
10	2.33	2.39	2.31	15.1	2.21	13.8
20	2.23	2.26	2.22	29.1	2.17	12.0

* Values estimated from extrapolation.

Fig. 11. Compositional dependence of some optical properties of $(100-3x)\text{BiO}_{1.5}\cdot x\text{BaO}\cdot 2x\text{CuO}$ glasses. (a) n_d and n_{∞} ; (b) R_m .

$$R_m = V_m \frac{n_{\infty}^2 - 1}{n_{\infty}^2 - 1} \quad (8)$$

The ν_d values of the present glasses are in the range 13–30, classified into high dispersion glasses.

Figure 11 shows the compositional dependence of (a) n_d and n_{∞} and (b) R_m of $(100-3x)\text{BiO}_{1.5}\cdot x\text{BaO}\cdot 2x\text{CuO}$ glasses. It is found that the additivity completely holds for both n and R_m similarly to molar volume. It has been reported that the refractive index of thin $\alpha\text{-Bi}_2\text{O}_3$ film at 550 nm is 2.45.²⁵⁾ The refractive index of fictive Bi_2O_3 glass at 550 nm is estimated at 2.46 by extrapolation, agreeing with this value. This also supports that coordination environment around Bi^{3+} ions resembles that in $\alpha\text{-Bi}_2\text{O}_3$ crystal which is constructed by BiO_5 and BiO_6 polyhedra, which is also the case for $\text{BiO}_{1.5}\cdot\text{GaO}_{1.5}$ glasses.²³⁾

4.4 Thermal properties and glass structure in relation to copper valence

The $(T_x - T_g)$ in the present glasses shows the maximum at 55–60% of the $\text{Cu}^+ / (\text{Cu}^+ + \text{Cu}^{2+})$ ratio. This may be explained by the presence of Cu_4O_3 crystal-like clusters in the present Bi-Ba-Cu-O glasses. The *in situ* high-temperature XRD measurement indicated that Cu_4O_3 crystal is precipitated in $50\text{BiO}_{1.5}\cdot 25\text{BaO}\cdot 25\text{CuO}$ glass on heating,¹⁰⁾ although the

crystal is finally transformed to Cu₂O or CuO crystal. In Cu₄O₃ crystal the Cu⁺/(Cu⁺ + Cu²⁺) ratio is just 50% and Cu⁺ and Cu²⁺ ions form Cu-O-Cu colinear bond and CuO₄ square plain, respectively.²⁶⁾ Therefore, the amount of Cu₄O₃ crystal-like units may become maximum at about 50% of the Cu⁺/(Cu⁺ + Cu²⁺) ratio. The wide glass-forming region in the present system instead of high concentration of CuO may be attributed to the presence of complex Cu₄O₃ crystal-like structural units, increasing randomness of the system. Consequently, it seems reasonable that the Bi-Ba-Cu-O glasses may be most stable at about 50% of the Cu⁺/(Cu⁺ + Cu²⁺) ratio.

5. CONCLUSION

Some physical properties of BiO_{1.5}-BaO-CuO ternary glasses were investigated and they were correlated with glass structure. It was found that the glass structure depends on Cu⁺/(Cu⁺ + Cu²⁺) ratio rather than glass composition. It was assumed that the local structure around Bi³⁺ ions resembles that in α -Bi₂O₃ crystal. On the other hand, the Cu₄O₃ crystal-like units might be present in the present glasses.

REFERENCES

- (1) T. Komatsu, R. Sato, K. Imai, K. Matusita and T. Yamashita, *Jpn. J. Appl. Phys.*, **27**, L550-52 (1988).
- (2) T. Minami, Y. Akamatsu, M. Tatsumisago, N. Tohge and Y. Kowada, *Jpn. J. Appl. Phys.*, **27**, L777-78 (1988).
- (3) D.G. Hinks, L. Soderholm, D.W. Capone II, B. Dabrowski, A.W. Mitchell and D. Shi, *Appl. Phys. Lett.*, **53**, 1341-42 (1988).
- (4) F.H. Garzon, J.G. Berry and I.D. Raistrick, *Appl. Phys. Lett.*, **53**, 805-07 (1988).
- (5) Y. Abe, H. Hosono, M. Hosoe, J. Iwase and Y. Kubo, *Appl. Phys. Lett.*, **53**, 1341-42 (1988).
- (6) H. Zheng, R. Xu and J.D. Mackenzie, *J. Mater. Res.*, **4**, 911-15 (1989).
- (7) A. Inoue, H. Kimura, K. Matsuzaki, A.P. Tsai and T. Matsumoto, *Jpn. J. Appl. Phys.*, **27**, L941-43 (1988).
- (8) M. Tatsumisago and C.A. Angell, S. Tsuboi, Y. Akamatsu, N. Tohge and T. Minami, *Appl. Phys. Lett.*, **54**, L2268-70 (1989).
- (9) K.K. Som and B.K. Chaudhuri, *Phys. Rev.*, **41**, 1581-91 (1990).
- (10) F. Miyaji, T. Yoko and S. Sakka, *J. Non-Cryst. Solids*, **126**, 170-72 (1990).
- (11) F. Miyaji, S. Fujimine, T. Yoko and S. Sakka, *J. Non-Cryst. Solids*, **150**, 107-11 (1992).
- (12) R. Sato, T. Komatsu and K. Matusita, *J. Non-Cryst. Solids*, **134**, 270-76 (1991).
- (13) S. Sakka, F. Miyaji, S. Fujimine and T. Yoko, *Proc. XVI Int. Cong. Glass, Madrid, Vol. 2*, 53-58 (1992).
- (14) F. Miyaji, S. Fujimine, T. Yoko and S. Sakka, *Zairyo*, **42**, 478-83 (1993).
- (15) F. Miyaji, S. Fujimine, T. Yoko and S. Sakka, submitted to *J. Am. Ceram. Soc.*
- (16) S. Banerjee and A. Paul, *J. Am. Ceram. Soc.*, **57**, 286-90 (1974).
- (17) S. Sakka, K. Kamiya, K. Matusita and T. Tachi, *J. Ceram. Soc. Japan.*, **84**, 397-403 (1976).
- (18) S.P. Singh, G. Prasad and P. Nath, *J. Am. Ceram. Soc.*, **61**, 377-79 (1977).
- (19) M. Cable and Z.D. Xiang, *Phys. Chem. Glasses*, **30**, 237-242 (1989).
- (20) H. Zheng, M.W. Colby and J.D. Mackenzie, *J. Non-Cryst. Solids*, **127**, 143-50 (1991).
- (21) F.G.K. Baucke, J.A. Duffy, *Phys. Chem. Glasses*, **32**, 211-18 (1991).
- (22) G. Malmros, *Acta Chem. Scand.*, **24**, 384-96 (1970).
- (23) F. Miyaji, T. Yoko, J. Jin, S. Sakka, T. Fukunaga and M. Misawa, *J. Non-Cryst. Solids*, in press.
- (24) S.H. Wemple, *J. Chem. Phys.*, **67**, 2151-68 (1977).
- (25) "Thin Film Handbook", Ed. by Japan Society for the Promotion of Science 131st Committee, Ohm-sha, pp. 820 (1983).
- (26) M. O'Keeffe and J.-O. Bovin, *Am. Mineral.*, **63**, 180-85 (1978).